

Wearable Roller Rings to Enable Robot Dexterous In-Hand Manipulation through Active Surfaces

Hayden M. Webb¹, Podshara Chanrungmaneekul¹, Shenli Yuan², and Kaiyu Hang¹

Abstract—In-hand manipulation is a crucial ability for reorienting and repositioning objects within grasps. The main challenges are not only the complexity in the computational models, but also the risks of grasp instability caused by active finger motions, such as rolling, sliding, breaking, and remaking contacts. Based on the idea of manipulation without lifting a finger, this paper presents the development of Roller Rings (RR), a modular robotic attachment with active surfaces that is wearable by both robot and human hands. By installing and angling the RRs on grasping systems, such that their spatial motions are not co-linear, we derive a general differential motion model for the object actuated by the active surfaces. Our motion model shows that complete in-hand manipulation skill sets can be provided by as few as only 2 RRs through non-holonomic object motions, while more RRs can enable enhanced manipulation dexterity with fewer motion constraints. Through extensive experiments, we wear RRs on both a robot hand and a human hand to evaluate their manipulation capabilities, and show that the RRs can be employed to manipulate arbitrary object shapes to provide dexterous in-hand manipulation.

I. INTRODUCTION

To physically engage robots with our daily tasks, evolving new modalities of in-hand manipulation skills is crucial for addressing problems associated with the traditional manipulation paradigms. In the past decades, extensive studies have worked towards improving in-hand manipulation by developing new hand designs, computational models, and more integrated systems to not only mechanically provide better options, but also computationally and perceptually enhance their manipulation capabilities [1]–[3].

Typically, in-hand manipulation is performed using precision grasps due to its robust dexterity. However, such hand-object configurations can come at the cost of stability and strength as limited by the small contacts at the fingertips. Moreover, due to the high degrees of freedom, precision grasp-based manipulation often relies on computationally complex, small-scale, and vulnerable movements to perform basic manipulations. Finger-gaiting, for example, requires the breaking of contacts to perform manipulations, which in turn compromises the grasp's total stability. In contrast, using power grasps is more stable but typically lacks the capability to perform the necessary relative motions between the object and hand. In-hand manipulation, in essence, is about stably maintaining and moving contacts with the manipulated object, but most traditional approaches fail to encompass both of these values.

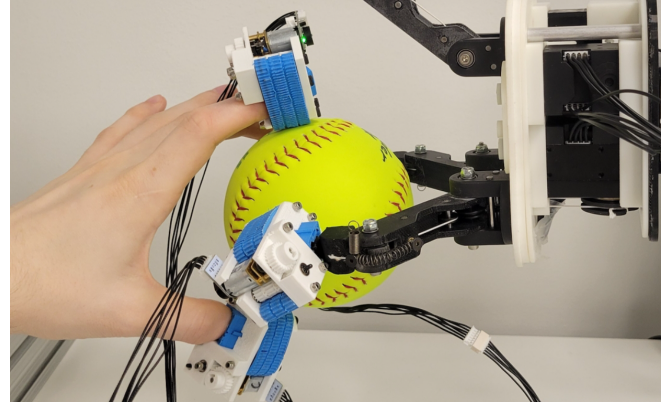


Fig. 1. Four Roller Rings, affixed on both a robot hand and a human hand, that are co-grasping a softball. Configurations like these can enable in-hand human-robot co-manipulation for grasped objects.

To this end, a number of novel robot hands have been developed to fill in the aforementioned gaps. To mitigate the concerns of grasp stability, underactuated hands have been designed to enable passive stability maintenance, while requiring significantly less degrees of control to be regulated for in-hand manipulation [4]. Yet, such designs are limited to very small-scaled manipulation when utilizing manipulation techniques, such as finger-gaiting [5], due to their high complexity and ability to easily lose stability. Alternatively, palm support-based manipulation has been explored through compliant hand controls to greatly enlarge the manipulation ranges [6]–[8], however, without much consideration of the manipulation precision.

Being an unconventional alternative, the concept of active surfaces [9], which actively moves a grasp contact by directly translating the contact on the robot hand (for example, via a conveyor belt), has created a new modality for in-hand manipulation. Robot hands with active surfaces are capable of performing dexterous manipulation *without lifting a finger* and, in theory, can translate the contacts without any limits as opposed to finger-gaiting. For rigid hands, motions actuated by active surfaces need to be precisely controlled to maintain the grasp stability [10], [11]. Recently, the BACH hand designed by our team has further combined mechanical compliance and active surfaces into a hand design [12], enabling unprecedented in-hand manipulation skills without requiring complex computational models or control schemes. However, a major limitation of the BACH is that its capability cannot be directly transferred to any other hand design. Likewise, most active surface-based solutions develop their systems

¹Department of Computer Science, Rice University, Houston, TX 77005, USA. ²Department of Mechanical Engineering, Stanford University, Stanford, CA 94305, USA. This work was supported by NSF award FRR-2240040.

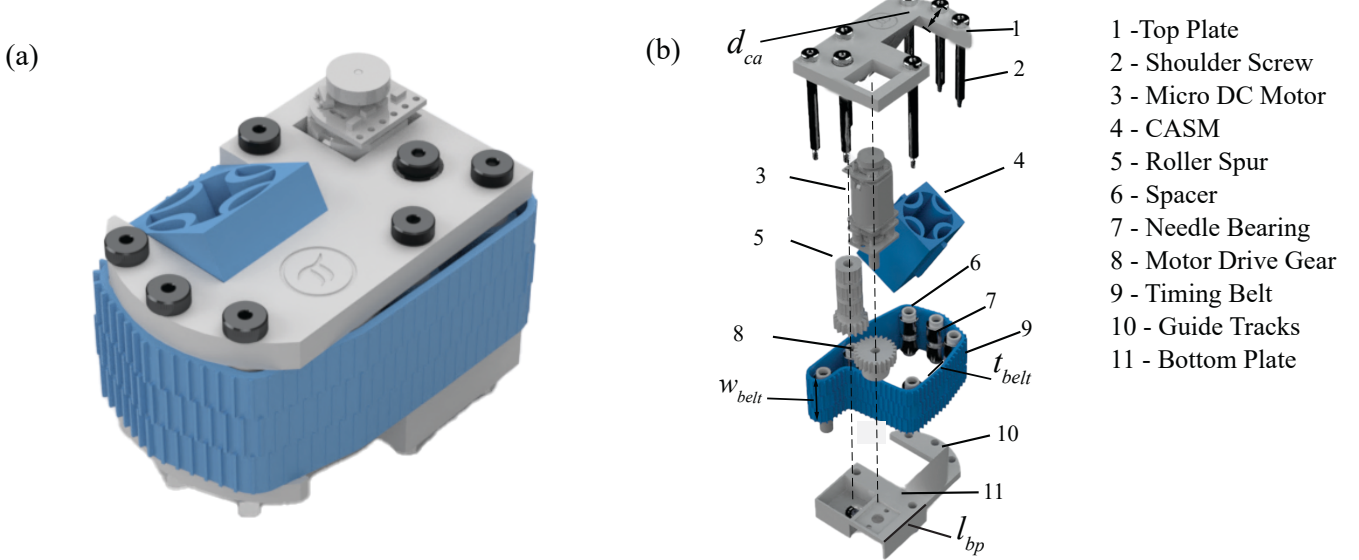


Fig. 2. CAD Model of the Roller Ring: (a) Render of the fully constructed device as seen in Fig. 1. (b) exploded view of the device with angled guide tracks and active surfaces. Dimensions of each specified variable can be found in Table I

with this technique integrated into itself rather than having it be integratable into the system.

To this end, we, in this work, propose the design of the Roller Rings (RR) (exemplified in Fig. 1) – a new form of wearable devices that can enable and augment active surface-based in-hand manipulation for *any hands* due to its modularity. In brief, this work provides:

- 1) The world’s first wearable device for manipulation augmentation that is low-cost and easy to fabricate;
- 2) A complete manipulation solution through differential manipulation motions (Sec. IV);
- 3) A manipulation device attachable to any robot and human hands while not changing the existing capability of the original hands.

We discuss related research in Sec. II, and then describe the design principles for the Roller Rings in Sec. III. In Sec. IV, we derive the differential motion model for the RR-based in-hand manipulation. Real-world experiments with both robot and human hands are discussed in Sec. V. Finally, Sec. VI concludes and discusses the future work.

II. RELATED WORK

In the past decades, a large number of robot hands have been developed to carry out dexterous manipulation [3]. The Stanford/JPL hand [13] and the Utah/MIT hand [14], for example, are among the earliest hands with in-hand manipulation capabilities. Due to the fact that a number of robot hands are inspired by human hands, common human manipulation techniques such as finger-gaiting became a natural choice for robot manipulation [5], [15]–[17]. During finger-gaiting, robot fingertips will sequentially break and remake contacts, essentially allowing fingers to “walk” along the grasped object to perform manipulation. However, fingertip movements are always challenged by grasp stability and

limited to small motion scales. Different from the finger-gaiting approach, rolling manipulation [18]–[20] allows the grasped object to be moved in-hand without the need for breaking contacts, enabling simpler controls and more stable manipulation. This approach, however, is still challenged by the very small scale of in-hand object motion ranges.

A. Rolling Manipulation and Active Surfaces

Robot grippers with active surfaces [10]–[12], [21]–[23] are specifically designed to perform rolling manipulation. These grippers have shown their unique abilities in various in-hand manipulation tasks, as they allow the grasped object to be manipulated without the need to lift fingers during manipulation. The velvet finger [21], for example, utilizes a set of actuated fingers inlaid with active surfaces to perform both rotational and translational manipulation. Additionally, the Roller Grasper V2 [11] has active surfaces designed into its fingertips to dexterously grasp and manipulate objects with the combination of roll & pitch movements. A more recent work [12] demonstrated that active surfaces and mechanically compliant grasps can be used to dexterously manipulate objects without any complex computational models or control schemes. While not specified in [12], the active surfaces in this work have fixed directions and were used differentially to generate various net object motions. Although these aforementioned designs have shown their improved in-hand manipulation capabilities, their designs do not generalize to or enhance the capabilities of any existing hand designs.

B. Algorithmic Approaches to Active Surfaces

Computational models have been derived to search for the optimal combinations of active surface motions to enable in-hand manipulation. For example, [24] samples certain grasps using object mesh models to generate object rotations. Using

TABLE I
MODEL SPECIFICATIONS OF THE ROLLER RING (FIG. 2, 3)

Symbol	Description	Value
d_{ca}	Distance to Contact Area [mm]	6
w_o	Outer Width of CASM [mm]	17
w_{ih}	Inner Width of Human CASM [mm]	12
w_{io}	Inner Width of Model O CASM [mm]	8
w_{belt}	Width of Timing Belt [mm]	18
t_{belt}	Thickness of Timing Belt [mm]	0.5
l_{bp}	Length of Backpack [mm]	20

this approach, the sum of combinations of angular velocities is standardized to actuate the in-hand motions of the grasped object. [25], [26] used a vision-based control system to determine the geometric information of an object in the next frame and calculated the necessary control commands of the active surface motions to achieve it. Additionally, employing control over both the belts and fingers greatly increases the flexibility of the active surface-based manipulation, while at the cost of more complex hand-object models [11]. However, the existing algorithms are all designed in an *ad hoc* manner to only work for specific designs. In this work, we derive a general motion model for active surface-based in-hand manipulation to unify the formulation of such manipulation skills (See Sec. IV). Based on this motion model, we show that our proposed RRs are capable of providing a complete set of non-holonomic in-hand skills with as few as 2 RRs, and that more RRs can be employed to improve the dexterity and robustness of the manipulation.

III. DESIGN

While active surfaces have shown promising capabilities for in-hand manipulation tasks, previous manipulation systems with active surfaces are limited to their underlying hand designs. In this work, we aim to improve the manipulation capabilities of existing robot hands through the wearable and modular Roller Rings (RR). With the integration of the RRs, robot hands that are designed for various grasping and manipulation purposes with different form-factors will have the ability to manipulate grasped objects without breaking contacts (i.e. lifting their fingers). To achieve this goal, we propose the following design principles:

- 1) The design should provide a full spatial manipulation capability, i.e., moving a grasped object from an arbitrary initial pose to an arbitrary target pose within the workspace;
- 2) The RRs should have a relatively compact form factor allowing them to be operated without compromising the grasping ability of the hand that the RRs are mounted on;
- 3) The RRs should be customizable in order for them to adapt to a wide range of robot hands and fingers.

A. Components

A CAD model of the RR is presented in Fig. 2 and the dimensions can be found in Table I. The top and bottom plates of the RR were 3D-printed using Polylactic Acid

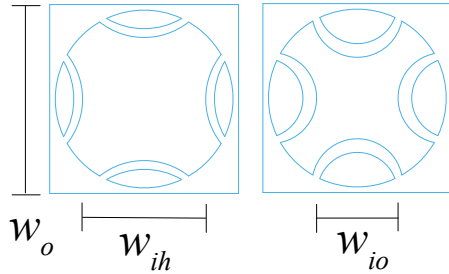


Fig. 3. CASM Variants for Roller Ring as given by Table I(Left to Right: Human Hand Variant, Yale Model O Hand Variant) Dimensions of each specified variable can be found in Table I.

(PLA, Bambu PLA Basic) at 30% infill on a Bambulab X1-Carbon 3D Printer and the actuated timing belt & CASM were 3D-printed using Thermoplastic Polyurethane (TPU, NinjaTek Chinchilla 75A).

Each RR variant has a one degree of freedom (DoF) active surface that is achieved using a timing belt routed through a series of needle bearings. The single DoF design is used as opposed to the 2-DoF (pivot and roll) design in [10], [11] to minimize the form factor of the RR in accordance with the guiding principles. Without the additional pivot joint, multiple RRs need to be used simultaneously and differentially in order to generate a net motion for the grasped object (see Sec. IV).

The belt is driven by a Micro DC Motor (N20 Gear Motor with 12CPR Encoder, 210:1 Gear Ratio) through a roller spur. It was routed, as seen in Fig. 2(b), to minimize the footprint of the whole RR model while satisfying the following constraints: (1) The timing belt forms a convex active surface where the object is contacted, and (2) The belt has enough contact area with the roller spur to avoid the teeth skipping when operated. The surface pattern of the outer side of the timing belt is designed to mate with the roller spur's teeth, which also doubles as a high friction surface for grasping and manipulation. Concurrently, it has grooves on the inner side to fit onto the needle bearings and to constrain the lateral motion, similarly to [12].

The RR can be mounted on various grasping systems through a customizable Conformable Affixing Sleeve Module (CASM) mounted on the Guide Track of the RR. To ensure that the device was generally wearable by any form of grasping system and abide by the guiding principles, we decided to employ the use of an inverted quatrefoil as seen in Fig. 2(b)(4). This was chosen due to its ability to resist plastic deformation under high tension due to the combination of the filament and geometry's innate compliance [27]. This compliance ensured that when we put the RR on a grasping system, the interior correctly deformed to hold itself in place without long term degradation. This high level of compliance allowed for the CASM to be utilized in both the robot and human tests when using the designed variants for both grasping systems (Fig. 3). The CASM variants seen in Fig. 3 were designed following these constraints: (1) The outer width of the CASM (w_o) had to be at least 2mm greater

than the greatest width of the attachment point for the set of utilized grasping systems, (2) the quatrefoil's fins had to be at least 1mm thick, and (3) the inner width (w_i) had to be at least 2mm less than the attachment point. In following these parameters, the CASM variants would correctly deform to the different grasping systems while still being attachable to the same RR. We chose a w_o of 17mm due to the human finger having the greatest width of the set at 15mm, then parameterized the set of CASM's from this baseline. Further demonstration of the CASM can be found in Section V

B. Angled Active Surface

The design principle (1) specifies that the RR be capable of performing full spatial manipulation. Considering parallel finger configuration is very common in multi-fingered grasping and manipulation, we designed the active surface to be angled from the axis of the finger the RR is mounted on (Fig. 2(b)(10)). In a simplified model, the active surface can be considered as a belt rotating around an axis of the CASM wherein this tilted design reduces the likelihood of the situation where the rotation axes of multiple RRs are parallel. The drawback of the tilted angle design is the increased footprint of the RR that comes with the larger angle. However, the design is generated in a way for the tilted angle to be easily changeable based on the specific grasping system used. If only two RRs are used, the active surfaces of the two RRs arranged orthogonally will maximize the manipulability of the system. As a proof of concept, we empirically selected a 30° angle between the active surface and the CASM to balance the performance and form factor of the design. Further discussion of this theorem can be found in Section IV and the evaluations of this can be found in Section V.

IV. MOTION MODEL

In this section, we derive a general motion model for active surface-based in-hand manipulation. We show that a complete in-hand manipulation skill set can be provided by as few as 2 active surface contacts through non-holonomic object motions, and that more active surface contacts can further improve the manipulation flexibility. We start with deriving a motion model that focuses on the in-hand rotation of a unit sphere, and then extend this model to the in-hand rotation of arbitrary object shapes. Thereafter, we derive an in-hand translation motion model, which can be combined with the rotation motion model to provide a complete set of in-hand manipulation solutions.

A. In-hand Rotation of A Unit Sphere

Let us begin by assuming the manipulated object is a unit sphere object \mathbb{S}^2 . By making a contact with an active surface at a point $p_a \in \mathbb{S}^2$, as illustrated in Fig. 4, the linear motion of the active surface at this contact will generate a torque to this sphere with respect to its center:

$$\tau_a = p_a \times F_a^t \quad (1)$$

where $F_a^t \in \mathbb{R}^3$ is the tangential friction force at point a , as determined by the contact normal force $F_a^n \in \mathbb{R}^3$ and

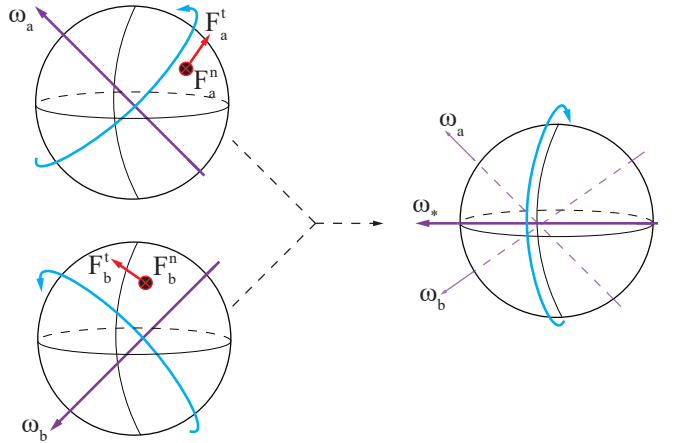


Fig. 4. In-hand rotation motion model for a unit sphere visualized with 2 active surface contacts. *Left:* angular velocities ω_a and ω_b can be independently actuated by active surfaces moving at points p_a and p_b . *Right:* When both contacts are simultaneously actuating the rotation of the object, the object's angular velocity is determined by a weighted sum of ω_a and ω_b as given by Eq. (7). Shown is an example where both contacts have the same weight.

the friction coefficient $\mu \in \mathbb{R}$: $|F_a^t| \leq \mu |F_a^n|$. Note that, as it will be discussed later, depending on the *relative linear motion* between the active surface and the sphere at p_a , the direction of the force F_a^t can vary, but the magnitude will stay constant when the two contacting surfaces are “slipping or scratching” against each other.

With this single active surface contact that moves with a linear velocity $v_a \in \mathbb{R}^3$, the sphere object will accelerate the rotation to synchronize its motion at the point p_a until the two surfaces in contact do not slip, resulting in an angular velocity of the object ω_a that satisfies:

$$v_a = \omega_a \times p_a \quad (2)$$

where $\omega_a = \hat{\omega}_a \dot{\theta}_a \in \mathbb{R}^3$ is expressed by an angular velocity $\dot{\theta}_a \in \mathbb{R}$ and an axis of rotation $\hat{\omega}_a = \frac{\omega_a}{|\omega_a|}$. Similarly, if there is a single active surface contact $p_b \in \mathbb{S}^2$ that moves at a speed of $v_b \in \mathbb{R}^3$, the angular velocity caused by this contact alone is ω_b that satisfies $v_b = \omega_b \times p_b$. Both cases are exemplified on the left in Fig. 4.

Now, if both contacts p_a and p_b are made with active surfaces, the sphere object will then initially start rotating still with “slipping” contacts. However, unless the two active surface motions are co-linear (in terms of the rotation axes), the resultant or converged motion at equilibrium will still be “slipping” to balance between the torque differences generated by the two contacts. To derive the object motion model based on the motions of these two active surface contacts, our goal is to find the angular velocity ω_* of the object when all “scratching or slipping” forces are balanced. The linear velocity of the sphere object at the contacts are:

$$v_a^* = \omega_* \times p_a, \quad v_b^* = \omega_* \times p_b, \quad (3)$$

which are different from the linear velocities v_a and v_b of the two active surface contacts. As discussed above, this will cause “slipping motions” at both contacts, where the motions

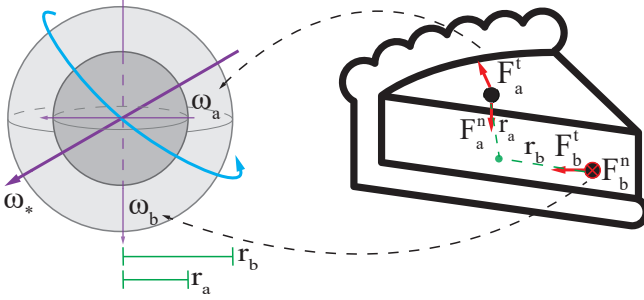


Fig. 5. Illustration of the multi-sphere model for rotating arbitrary objects in-hand with active surface contacts. Right: two active surface contacts p_a and p_b on a pie-shaped object. Left: an equivalent view of the physical effect of these two contacts visualized on two virtual spheres of radii r_a, r_b .

of the active surfaces relative to the object are given by $v_a - v_a^*$ and $v_b - v_b^*$. Such slippage will result in tangential forces at the contacts aligned to the relative motion directions:

$$\begin{aligned}\tau_a^* &= p_a \times (\mu |F_a^n| \frac{v_a - v_a^*}{|v_a - v_a^*|}) = k_a p_a \times (v_a - v_a^*) \\ \tau_b^* &= p_b \times (\mu |F_b^n| \frac{v_b - v_b^*}{|v_b - v_b^*|}) = k_b p_b \times (v_b - v_b^*)\end{aligned}\quad (4)$$

where $k_a = \frac{\mu |F_a^n|}{|v_a - v_a^*|}$ and $k_b = \frac{\mu |F_b^n|}{|v_b - v_b^*|}$ are scalar scaling factors determined by the magnitudes of both the contact forces and the relative velocities. When the object motion is at equilibrium (i.e. there is zero effective torque applied by the contacts) its motion will stabilize and the torques at both contacts should satisfy $\tau_a + \tau_b = 0$, yielding:

$$k_a p_a \times (v_a - v_a^*) = -k_b p_b \times (v_b - v_b^*) \quad (5)$$

since $\omega = p \times v$, we have:

$$k_a (\omega_a - \omega_*) = -k_b (\omega_b - \omega_*) \quad (6)$$

where ω_a and ω_b are the angular velocities independently generated by the contacts. Rearranging the former, we obtain the expression of the object's angular velocity:

$$\omega_* = \frac{k_a \omega_a + k_b \omega_b}{k_a + k_b} \quad (7)$$

From Eq. (7), we can see that the angular velocity of the sphere object, as simultaneously actuated by 2 active surfaces, is simply a weighted sum of the angular velocities of the object when it is actuated by each contact independently. Interestingly, the weights k_a and k_b are determined by the contact force and the intrinsic velocities of the active surfaces themselves. In other words, the difference between the velocities of the active surfaces will directly determine the object's motion ω_* . As such, our motion model is a *differential motion model*. Intuitively, we know that if we want to rotate the object with motions more biased by a contact, it can be done by increasing the contact force or by speeding up the corresponding active surface. Fig. 4 shows an example of when two contacts are simultaneously actuated by active surfaces with the same velocity & contact force.

Additionally, assuming non-collinear configurations of the active surfaces, we can see that the object's motion can be

activated to rotate about multiple, essentially infinite number of axes of rotation. As proven in [5], as long as a hand-object system can rotate an object about at least 2 orthogonal axes, the object can be reoriented from any angle to any other angle. Although the set of axes of rotation generated by Eq. (7) cannot guarantee to contain orthogonal axes, the axes generated can be projected to provide rotations about orthogonal pairs of axes. Therefore, it is evident from Eq. (7) that, with as few as only 2 active surfaces, it can provide a *complete* rotational manipulation solution. However, still due to the lack of guarantees for a pair of orthogonal axes of rotations, the generated motions are not necessarily able to travel in arbitrary directions of rotation, rendering the corresponding rotation-based manipulation solution a *non-holonomic* motion system that necessitates the object to often take “detours” from its current orientation to reach its goal orientation.

Furthermore, it is straightforward to extend Eq. (7) to N active surface contacts. We omit the derivation steps here, which are similar to the above, and directly write down the motion model:

$$\omega_* = \frac{\sum_{i=1}^N k_i \omega_i}{\sum_{i=1}^N k_i} \quad (8)$$

With more active surface contacts, Eq. (8) will be able to provide more axes of rotation, reducing the “detours” taken by the object to reach its goals.

B. Multi-Sphere Motion Model for Arbitrary Object Shapes

Extending from the rotation motion model on a unit sphere, we now model the rotations of arbitrary object shapes as actuated by active surface contacts. Let us still begin with the scenario with 2 contacts p_a and p_b on an object. However, this time the contacts are not necessarily on a unit sphere \mathbb{S}^2 . Their distances to the axis of rotation are represented by $r_a, r_b \in \mathbb{R}$. Intuitively, these two contacts are actuating the object as if there were 2 different spheres for them to make contacts, as illustrated in Fig. 5. As such, the torques generated by these two contacts, as shown in Eq. (9), are now additionally scaled by r_a, r_b :

$$\begin{aligned}\tau_a^* &= r_a k_a p_a \times (v_a - v_a^*) \\ \tau_b^* &= r_b k_b p_b \times (v_b - v_b^*)\end{aligned}\quad (9)$$

As such, similarly to the derivation for the motion model on a unit sphere, the torques should all balance out when the object is rotating at an equilibrium state. Skipping the intermediate steps, we can obtain the rotation motion model for N active surface contacts on arbitrary objects:

$$\omega_* = \frac{\sum_{i=1}^N r_i k_i \omega_i}{\sum_{i=1}^N r_i k_i} \quad (10)$$

Based on this multi-sphere motion model, Eq. (10) also provides a *complete and non-holonomic* rotational manipulation solution. However, a major difference now is that the individual angular velocities are additionally weighted by the distances between the contact and the rotation axis, providing another dimension for rotations to be regulated by contact variances.

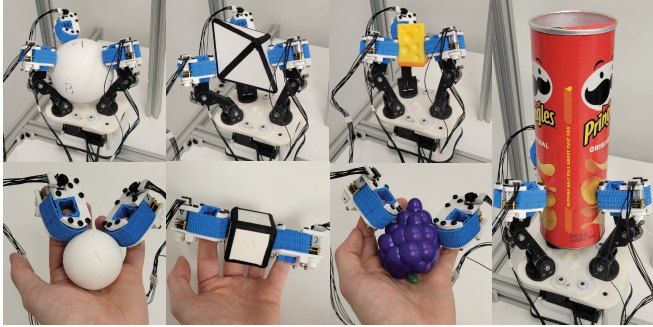


Fig. 6. Experimental Objects manipulated using the Roller Rings with the Yale Model O (Top Row Left to Right: A-F Sphere, Octahedra, Children’s Cheese Toy, Cardboard Tube; Bottom Row Left to Right: A-F Sphere, Cube, Children’s Grape Toy)

C. Motion Model for In-hand Translations

To achieve a complete in-hand manipulation solution, the final component required in our motion model is the ability to translate the object in-hand. Our model analysis here will focus on pure translations supplementary to the rotation models derived above. In practice, however, the object rotation and translation can happen simultaneously during manipulation in order to perform more efficient actions.

For pure in-hand object translation, the first requirement is that the object’s angular velocity should be zero. Based on our model above, we know this can be expressed as a motion constraint among all active surfaces: $\omega_* = \sum_{i=1}^N r_i k_i \omega_i = 0$. When this constraint is satisfied, which can be achieved in an infinite number of ways when multiple contacts exist to cancel out each other’s torques, the velocity of the object is purely determined by the linear forces provided by the active surfaces. Let us denote by $v^* \in \mathbb{R}^3$ the linear velocity of the object, by $v_i \in \mathbb{R}^3$ and F_i^t the linear velocity and the tangential force at the i -th active surface. The following equation further constrains the object’s translation:

$$\sum_{i=1}^N F_i^t \cdot \frac{v_i - v^*}{|v_i - v^*|} \cdot \frac{v_i \times v^*}{|v_i \times v^*|} = 0 \quad (11)$$

In Eq. (11), the tangential force at each contact is first aligned to the direction of the “slipping or scratching” motion and then projected to the perpendicular direction of the object’s motion (by dot product). The zero-sum of all these forces guarantees that the object is purely translating in the direction of v^* . In practice, although it is not difficult to obtain $\omega_* = 0$ as discussed above, achieving arbitrary translation motions is challenging due to the additional constraint (Eq. (11)), especially when the number of contacts is small. Nonetheless, given our complete solution of in-hand rotation, we will be able to manipulate the object from any pose to any others by sequencing translation and rotations. As shown in [28], a manipulation graph can be constructed to generate such action sequences, although the aforementioned “detours” are not avoidable.

V. EXPERIMENTS

To evaluate the design and motion model of the RR, we constructed a prototype, as seen in Fig. 2(a) to test its in-hand manipulation capabilities using various objects (Fig. 6). The RRs were affixed to both a Yale Model O hand and a human hand for all experiments wherein all experiments were conducted using teleoperation. As shown in Sec. III, each RR variant has one actuated DoF from the Micro DC Motor that was controlled using velocity control. Each RR had its velocity set to a differing set of values during the experiment so that the combinations of varying velocities can generate differential motions for the grasped object, thus allowing for a complete manipulation solution (Sec. IV).

A. Rotational Manipulation

While conducting the experiments, we evaluated the range of rotation that was physically possible by the RRs through their combined set of actuated DoFs. In this, so long as the manipulated object’s geometry didn’t collide internally with the grasping system and a stable grasp was maintained, we aimed to confirm that the designed RRs could rotate a grasped object from any initial orientation to any other goal orientation, so as to verify our theory derived in Sec. IV.

First, based on the single-sphere motion model, the A-F Sphere was grasped and manipulated by the Yale Model O Hand (Fig. 7(a)). We see that with 3 RRs, the sphere could be rotated to any face. Additionally, the rotations could be done about multiple axes, as opposed to the limited differential motions provided by 2 RRs as discussed in Sec. IV. The Cheese toy could also be rotated to any desired orientations, as shown in Fig. 7(c), physically justifying the in-hand rotation capability of our RR design, as well as the correctness of our multi-sphere motion model. Furthermore, we found that the form of grasping system used (i.e. Yale Model O Hand and Human hand) made no difference in the ability to fully rotate the grasp objects. Interestingly, as discussed by our motion models and better visualized in the supplementary video, “detours” were often needed for in-hand rotations since the RRs can only provide differential non-holonomic manipulation.

B. Translational and Rotation Manipulation

After confirming the ability of a full range of reorientation, we moved towards testing the translational manipulation of the RRs. Utilizing the translational portion of the Motion Model (Section IV) we were able to generate translations along all cardinal planes from the base set of actuated RRs. Following the same constraints as the rotational manipulation, so long as the object is stably grasped and does not collide internally with the hand, translations can be generated. Fig. 7(b-d) are examples showing both translations and rotations generated for grasped objects, including a Pringles tube, a Cheese toy, and a cube, to move them within the grasping system. We observed that, similarly to the rotational manipulation, the form of grasping system made no difference whether the RRs were affixed to a human or robot grasping system in terms of manipulation

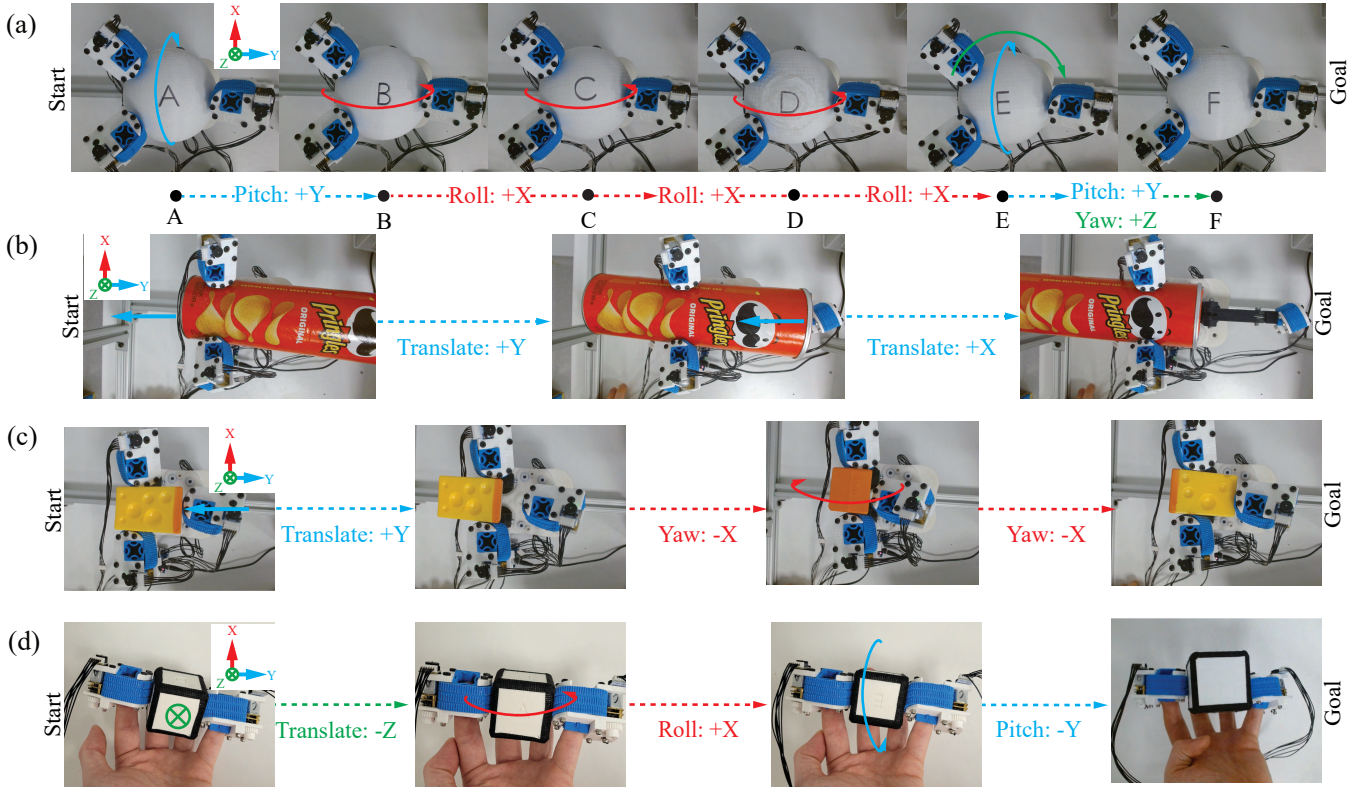


Fig. 7. Motion Examples of the RR: (a) A-F Sphere reoriented by the RR through all faces when held in a power grasp by the Yale Model O (b) Cardboard tube translated along the Yale Model O when held in a power grasp

capabilities. So long as the grasping constraints were met, rotations and translations can be generated in sequences to fully manipulate the in-hand object from any pose to any others, as discussed in Sec. IV, although as the same as before, often taking “detours”.

C. Object Variance

When running the experiments for the RRs, we evaluated how the difference in object geometries affected the manipulation capabilities of the RRs. When affixed to the Yale Model O Hand, we saw that larger objects were capable of being easily manipulated. Objects such as the A-F Sphere and Cube (6) could be smoothly manipulated when held in a power grasp. Sharp corners were difficult to manipulate around as they would push against the contact points when rotated about an axis normal to the set. However, the compliance of the Model O allowed for the RR to complete its manipulation tasks by accounting for the deflection. Objects of smaller geometries (i.e. children’s toys) were more difficult to manipulate as they could only be held in a precision grasp. This loss of stability decreased the ability of the Model O to stably hold the objects during manipulation.

This issue was mirrored when the RR was affixed to a human hand. Objects of smaller geometries (i.e. children’s toys) could be easily manipulated when held in a power grasp, sharp corners increased the difficulty of the grasp, and the compliance of human fingers improved the in-hand manipulation capabilities of the RR. Larger objects, however,

could only be grasped in a precision grasp. This increased the difficulty of the in-hand manipulation through a reduction in the stability. Overall, object variance between the relative geometry to the grasping system played a key factor in the ability to successfully and easily manipulate. Objects that were capable of being held in a power grasp were held stably and would not encounter loss of contact or slippage when performing in-hand manipulation.

D. Limitations of Roller Rings

1) *Geometric Constraint:* Due to the geometry of the RR and its attachment to the grasping system, objects that are larger than the power grasp task-space or thinner than the formed gap are difficult to manipulate with the base DoF. These objects can be manipulated when held in a precision grasp, but only at a reduced in-hand manipulation capability. Utilizing the palm and fingers as a support in the manipulation of these objects improves the in-hand manipulation, but is not effective across all geometries due to the lack of active surfaces across them.

2) *Friction:* Because the angle of the CASM was fixed to 30° to enable a full set of manipulation abilities, the RRs require “slipping and scratching” motions perpendicular to its main motion axes as needed by manipulation actions. Such motions will not only make the system less energy-effective, but also can bring more uncertainties since friction is difficult to model. In addition, the system’s durability can be reduced due to constant “scratching”.

3) *Non-Compliance*: Due to the RRs not being compliant, contacts between the grasping system and object are difficult to maintain using the RRs alone. Compliant grasping systems such as the Yale Model O and human hands are required in order to perform stable in-hand manipulation. This is because their compliance allows for a higher level of stability when manipulating objects that is not possible with the independent RRs. Compliant mechanism can conform to an object's geometry in order to adaptively facilitate the manipulation. Without this, affixing the RRs to a non-compliant system will induce difficulties in performing in-hand manipulation as the contacts will be easily broken.

VI. CONCLUSION AND FUTURE WORK

This paper proposed the design of a wearable Roller Ring, based on the concept of active surfaces, that can be used to enhance the in-hand manipulation capabilities of existing hand designs. Active surface-based motion models were derived to show that active surface-based manipulation in general provides a differential and non-holonomic manipulation model. The motion model also proves that the proposed design is able to provide a complete manipulation skill set including in-hand rotations and translations. Experiments were performed to physically verify the manipulation capabilities of RRs. Different objects of varying sizes and geometries were manipulated to empirically validate the applicability of our design in daily manipulation tasks. In future work, we plan to mechanically make the RRs more compliant, as well as reduce the friction in differential motions. Computationally, based on the derived motion models, we will develop algorithms to provide general and optimized manipulation solutions to more hand designs.

REFERENCES

- [1] R. Calandra, A. Owens, D. Jayaraman, J. Lin, W. Yuan, J. Malik, E. H. Adelson, and S. Levine, "More than a feeling: Learning to grasp and regrasp using vision and touch," *IEEE Robotics and Automation Letters*, vol. 3, no. 4, pp. 3300–3307, 2018.
- [2] I. M. Bullock and A. M. Dollar, "Classifying human manipulation behavior," in *IEEE International Conference on Rehabilitation Robotics*. IEEE, 2011, pp. 1–6.
- [3] C. Piazza, G. Grioli, M. Catalano, and A. Bicchi, "A century of robotic hands," *Annual Review of Control, Robotics, and Autonomous Systems*, vol. 2, pp. 1–32, 05 2019.
- [4] K. Hang, W. G. Bircher, A. S. Morgan, and A. M. Dollar, "Manipulation for self-identification, and self-identification for better manipulation," *Science robotics*, vol. 6, no. 54, p. eabe1321, 2021.
- [5] A. S. Morgan, K. Hang, B. Wen, K. Bekris, and A. M. Dollar, "Complex in-hand manipulation via compliance-enabled finger gaiting and multi-modal planning," *IEEE Robotics and Automation Letters*, vol. 7, no. 2, pp. 4821–4828, 2022.
- [6] A. Bhatt, A. Sieler, S. Puhlmann, and O. Brock, "Surprisingly robust in-hand manipulation: An empirical study," *Robotics: Science and Systems*, 2021.
- [7] O. M. Andrychowicz, B. Baker, M. Chociej, R. Jozefowicz, B. McGrew, J. Pachocki, A. Petron, M. Plappert, G. Powell, A. Ray *et al.*, "Learning dexterous in-hand manipulation," *The International Journal of Robotics Research*, vol. 39, no. 1, pp. 3–20, 2020.
- [8] A. Pagoli, F. Chapelle, J. A. Corrales, Y. Mezouar, and Y. Lapusta, "A soft robotic gripper with an active palm and reconfigurable fingers for fully dexterous in-hand manipulation," *IEEE Robotics and Automation Letters*, vol. 6, no. 4, pp. 7706–7713, 2021.
- [9] P. Datseris and W. Palm, "Principles on the development of mechanical hands which can manipulate objects by means of active control," *Journal of Mechanisms Transmissions and Automation in Design*, vol. 107, 06 1985.
- [10] S. Yuan, A. D. Epps, J. B. Nowak, and J. K. Salisbury, "Design of a roller-based dexterous hand for object grasping and within-hand manipulation," in *IEEE International Conference on Robotics and Automation (ICRA)*. IEEE, 2020, pp. 8870–8876.
- [11] S. Yuan, L. Shao, C. Yako, A. Gruebele, and J. Jr, "Design and control of roller grasper v2 for in-hand manipulation," in *IEEE International Conference on Intelligent Robots and Systems (IROS)*, 10 2020, pp. 9151–9158.
- [12] Y. Cai and S. Yuan, "In-hand manipulation in power grasp: Design of an adaptive robot hand with active surfaces," in *IEEE International Conference on Robotics and Automation (ICRA)*, 05 2023, pp. 10 296–10 302.
- [13] J. K. Salisbury and B. Roth, "Kinematic and force analysis of articulated mechanical hands," 1983.
- [14] S. Jacobsen, E. Iversen, D. Knutti, R. Johnson, and K. Biggers, "Design of the utah/mit dextrous hand," in *IEEE International Conference on Robotics and Automation (ICRA)*, vol. 3. IEEE, 1986, pp. 1520–1532.
- [15] S. Leveroni and K. Salisbury, "Reorienting objects with a robot hand using grasp gaits," in *Robotics Research: The Seventh International Symposium*. Springer, 1996, pp. 39–51.
- [16] L. Han and J. C. Trinkle, "Dexterous manipulation by rolling and finger gaiting," in *IEEE International Conference on Robotics and Automation (ICRA)*, vol. 1. IEEE, 1998, pp. 730–735.
- [17] R. R. Ma and A. M. Dollar, "An underactuated hand for efficient finger-gaiting-based dexterous manipulation," in *2014 IEEE International Conference on Robotics and Biomimetics (ROBIO 2014)*, 2014, pp. 2214–2219.
- [18] D. J. Montana, "The kinematics of contact and grasp," *The International Journal of Robotics Research*, vol. 7, no. 3, pp. 17–32, 1988.
- [19] A. Bicchi and R. Sorrentino, "Dexterous manipulation through rolling," in *IEEE International Conference on Robotics and Automation (ICRA)*, vol. 1. IEEE, 1995, pp. 452–457.
- [20] P. Choudhury and K. M. Lynch, "Rolling manipulation with a single control," *The International Journal of Robotics Research*, vol. 21, no. 5–6, pp. 475–487, 2002.
- [21] V. Tincani, M. Catalano, E. Farnioli, M. Garabini, G. Grioli, G. Fantoni, and A. Bicchi, "Velvet fingers: A dexterous gripper with active surfaces," in *IEEE International Conference on Intelligent Robots and Systems (IROS)*, 10 2012, pp. 1257–1263.
- [22] R. Ma and A. Dollar, "In-hand manipulation primitives for a minimal, underactuated gripper with active surfaces," in *ASME International Design Engineering Technical Conferences and Computers and Information in Engineering Conference*, 08 2016, p. V05AT07A072.
- [23] J. Gomez-de Gabriel and H. Wurdemann, "Adaptive underactuated finger with active rolling surface," *IEEE Robotics and Automation Letters*, 10 2021.
- [24] G. Xie, R. Holladay, L. Chin, and D. Rus, "In-hand manipulation with a simple belted parallel-jaw gripper," *IEEE Robotics and Automation Letters*, vol. PP, pp. 1–8, 01 2023.
- [25] Y. Isobe, S. Kang, T. Shimamoto, Y. Matsuyama, S. Pathak, and K. Umeda, "Vision-based in-hand manipulation for variously shaped and sized objects by a robotic gripper with active surfaces," *IEEE Access*, vol. PP, pp. 1–1, 01 2023.
- [26] ———, "Vision-based in-hand manipulation of variously shaped objects via contact point prediction," in *IEEE International Conference on Intelligent Robots and Systems (IROS)*, 10 2023, pp. 8727–8734.
- [27] M. S. Azmi, R. Ismail, and R. Hasan, "Investigation on the static and dynamic behavior of bcc lattice structure with quatrefoil node manufactured using fused deposition modelling additive manufacturing," *IOP Conference Series: Materials Science and Engineering*, vol. 788, no. 1, p. 012008, apr 2020.
- [28] S. Cruciani, C. Smith, D. Kragic, and K. Hang, "Dexterous manipulation graphs," in *IEEE International Conference on Intelligent Robots and Systems (IROS)*. IEEE, 2018.